ELSEVIER

Ceramics International 30 (2004) 689–695

CERAMICS
INTERNATIONAL

www.elsevier.com/locate/ceramint

Dense ceramics of single-crystalline-phase osumilite synthesized by solid-state reaction

Yuichi Kobayashi*, Tomoji Takeda

Department of Applied Chemistry, Faculty of Engineering, Aichi Institute of Technology, 1247 Yachigusa, Yakusa, Toyota, Aichi 470-0392, Japan

Received 12 June 2003; received in revised form 27 June 2003; accepted 28 July 2003

Abstract

Solid-state reactions of ultrafine particles of magnesium hydroxide and barium carbonate with kaolin were investigated to obtain dense osumilite ceramics. Hexacelsian, μ-cordierite and α-cordierite were found to crystallize prior to the formation of osumilite above 1200 °C. Dense ceramics of single-crystalline-phase osumilite were obtained by a delicate compositional adjustment around the nominal formula of osumilite $2MgO{\cdot}BaO{\cdot}3Al_2O_3{\cdot}9SiO_2$, because it hardly showed any solid solution formation. Single-phase osumilite ceramics showed a linear thermal expansion coefficient of $2.7 \times 10^{-6}\,K^{-1}$ (RT–900 °C), a relative dielectric constant of 5.6 and a dielectric loss of 5×10^{-5} at 1 MHz. The osumilite ceramics prepared in the present work may fulfill the requirement from various applications.

Keywords: A. Sintering; B. Microstructure-final; C. Thermal expansion; D. Silicate

1. Introduction

Barium osumilite was discovered accidentally during attempts to improve the sintering characteristics of cordierite ceramics by addition of $BaCO_3$ [1]. The chemical composition of barium osumilite was estimated to be $2MgO{\cdot}BaO{\cdot}3Al_2O_3{\cdot}9SiO_2$ and the crystal structure [2] was composed of hexagonal double rings $(Si, Al)_{12}O_{30}$, connected by metal ions Al^{3+}, Mg^{2+}, and Ba^{2+}. Since the thermal expansion coefficient of barium osumilite (hereafter referred to osumilite) is low, which is attributable to its crystal structure similar to cordierite [3], osumilite ceramics may serve as promising refractory materials and thermal-shock resistant materials.

There are previous reports of whisker-reinforced ceramics [4] or ceramic-fiber reinforced ceramics [5,6] using osumilite as a matrix material. Sol–gel methods [7] and glass-ceramics [8,9] methods have been applied to develop dense osumilite ceramics as thermal-shock resistant materials. Unfortunately, single-phase osumilite ceramics have never been fabricated because hexacelsian or cordierite second phases could not be avoided.

Cordierite and Ba-celsian ($BaO{\cdot}Al_2O_3{\cdot}2SiO_2$) also have a low thermal expansion coefficient as well as low dielectric constant [10], so that these silicates are candidates of ceramic-fiber reinforced ceramics or substrate materials for high frequency electronic circuits. However, preparation of dense ceramics of these two materials is difficult. In case for cordierite, only expensive starting materials, such as alkoxides, enable the preparation of dense ceramics and in case for Ba-celsian, hexacelsian once formed sluggishly transforms into the monoclinic form, so that heat treatment temperature higher than 1400 °C and longer period is necessary.

In the present study, the preparation conditions for dense osumilite ceramics of single-crystalline-phase by solid-state reaction were established, and their dielectric properties and thermal expansion coefficient were determined.

2. Experimental procedure

2.1. Starting materials

New Zealand kaolin was wet-classified with diameter of less than 1 μm, and used in a wet state before drying. The

---

* Corresponding author. Tel.: +81-565-48-8121; fax: +81-565-48-0076.

E-mail address: kobayasi@ac.aitech.ac.jp (Y. Kobayashi).

0272-8842/$30.00 © 2003 Elsevier Ltd and Techna Group S.r.l. All rights reserved.
doi:10.1016/j.ceramint.2003.07.015

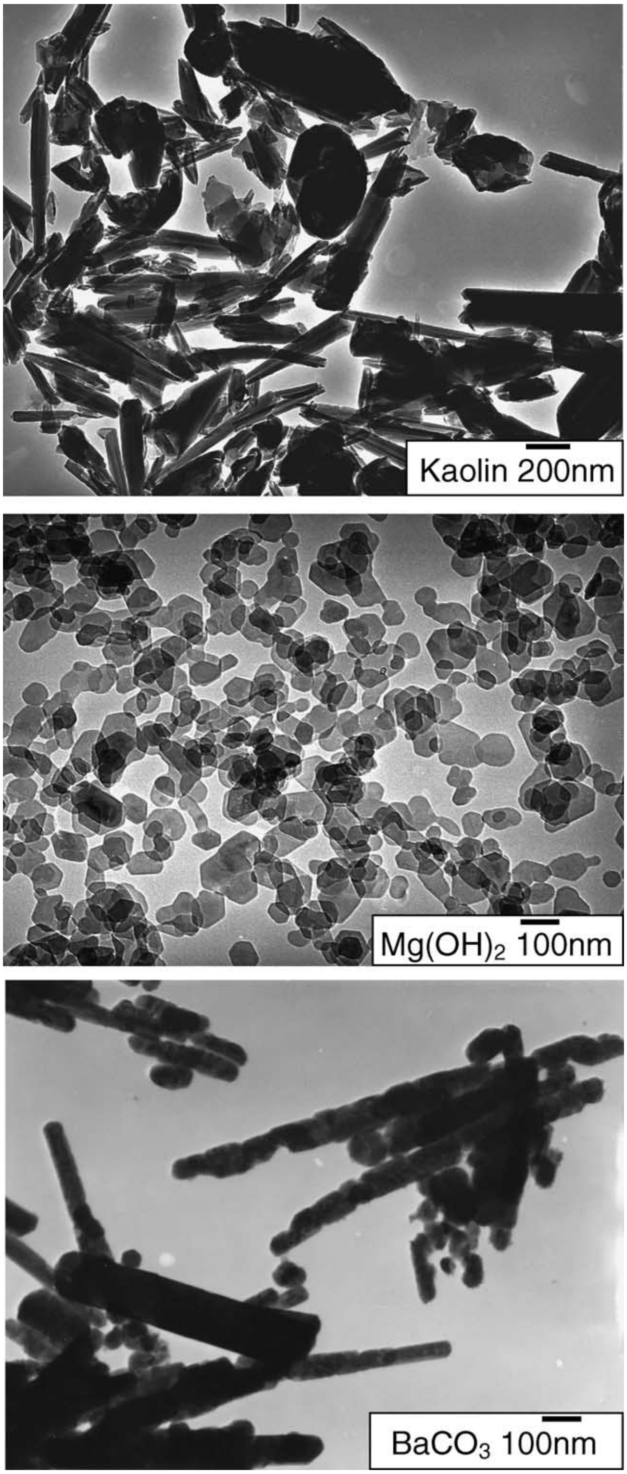

Fig. 1. TEM photographs of New Zealand kaolin, synthesized magnesium hydroxide and synthesized barium carbonate.

classified New Zealand kaolin is consisted of cylindrical halloysite particles with an average length of 0.6 μm and an average diameter of 0.1 μm, as shown in Fig. 1. The chemical composition of classified New Zealand kaolin (hereafter referred to kaolin) is as follows: SiO_2: 45.72%, Al_2O_3: 38.09%, Fe_2O_3: 0.25%, TiO_2: 0.08%, CaO: 0.01%, MgO: 0.08%, K_2O: 0.01%, Na_2O: 0.06%, Ig.loss = 14.05%. The molar ratio SiO_2/Al_2O_3 was 2.04, almost coincident with the theoretical composition of halloysite.

Ultrafine $Mg(OH)_2$ particles were precipitated from 200 ml of 0.25 mol/l magnesium chloride solution with 50 ml of 14.8 mol/l ammonia solution and separated by centrifugation. A photograph of the synthesized magnesium hydroxide observed by transmission electron microscope is shown in Fig. 1. The magnesium hydroxide particles were hexagonal tabular microcrystals with an average width of about 0.1 μm, and the thickness was estimated to be about 20 nm by X-ray line broadening.

Ultrafine $BaCO_3$ particles were precipitated from 300 ml of 0.32 mol/l barium chloride solution with 300 ml of 1 mol/l ammonium carbonate solution and separated by centrifugation. A photograph of the synthesized barium carbonate observed by transmission electron microscope is also shown in Fig. 1. Barium carbonate particles were cylindrical microcrystals with a length of about 1.0 μm, and a diameter of about 0.07 μm.

In order to prepare the mixtures of these raw materials to osumilite composition (SiO_2/Al_2O_3 molar ratio is 3), silica sol SN–O (Nissan Kagaku Kogyo, Tokyo, Japan) was added, because raw material kaolin had $SiO_2/Al_2O_3 = 2$.

2.2. Preparations

After the magnesium hydroxide, barium carbonate, kaolin and silica sol were weighed in a molar ratio of $(1-n)\mathrm{MgO}\cdot n\mathrm{BaO}\cdot\mathrm{Al_2O_3}\cdot m\mathrm{SiO_2}$, the mixtures were ultrasonically dispersed and dried slowly while being stirred in a mortar. Here, compositional parameters, n and m were individually altered from 0 to 1.0 and from 2.0 to 3.0, respectively. The specimen of $n = 0.333$ and $m = 3.0$ corresponded to nominal osumilite composition $2MgO\cdot BaO\cdot 3Al_2O_3\cdot 9SiO_2$. Fig. 2 indicates quaternary system in $MgO–BaO–Al_2O_3–SiO_2$, redrawn from “Phase Diagrams for Ceramists, 1964, p. 195, 246” [11]. Composition of osumilite lies on the line between hypothetical composition of $MgO\cdot Al_2O_3\cdot 3SiO_2$ (point A in Fig. 2, $n = 0$ and $m = 3$) and $BaO\cdot Al_2O_3\cdot 3SiO_2$ (point B in Fig. 2, $n = 1$ and $m = 3$). The compositions of cordierite ($2MgO\cdot 2Al_2O_3\cdot 5SiO_2$, $n = 0$ and $m = 2.5$) and celsian ($BaO\cdot Al_2O_3\cdot 2SiO_2$, $n = 1$ and $m = 2$) lie on a quadrilateral ABCD.

The mixed powders were uniaxially compressed at 98 MPa to form a disk, 16 mm in diameter. The green compacts thus prepared were heat treated in air from room temperature up to 1000 °C at a rate of 5 °C/min and at a rate of 2.5 °C above 1000 °C. After keeping at respective temperatures, the furnace was allowed to cool down.

2.3. Characterizations

The morphology of starting materials was observed by transmission electron microscope (TEM; JEOL, JEM-200,

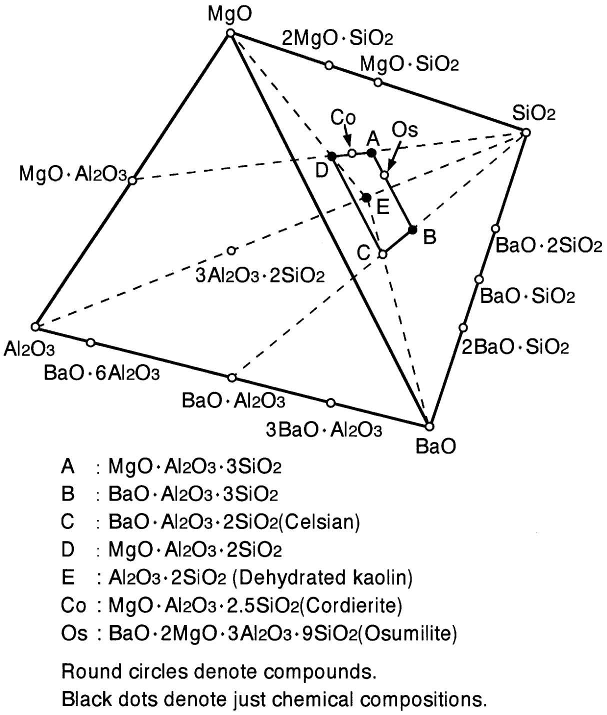

Fig. 2. Stable compounds and experimental compositions in the quaternary system, BaO–MgO–Al_2O_3–SiO_2. Redrawn from “Phase Diagrams for Ceramists, 1964, p. 195, 246” [11].

Tokyo, Japan). Crystalline-phases were identified by means of X-ray diffraction (Rigaku Denki, RAD-B, Tokyo, Japan) with Cu Kα radiation. X-ray intensity was determined by the diffraction peak heights of the phases listed in Table 1.

DTA and TG measurements were carried out using a DTA–TG apparatus (Rigaku Denki, TAS-100, Tokyo, Japan) at a heating rate of 10 °C/min. Thermal expansion coefficients of the sintered specimens were measured using TMA apparatus (Rigaku Denki, TAS-100, Tokyo, Japan) at a heating rate of 10 °C/min from room temperature to 900 °C. Bulk density and apparent porosity of fired specimens were determined by the Archimedes immersion technique in boiling water. The microstructures of the specimens were observed by a scanning electron microscope (SEM; JEOL, JSM-5310, Tokyo, Japan) on the polished surface.

Table 1
Miller indices and angles of X-ray diffraction peaks for measurement of crystal contents

Crystal	JCPDS number	(*h k l*)	Diffraction angle Cu Kα (°)
Ba-osumilite	16-402	(2 1 1)	27.6
α-Cordierite	13-293	(2 0 2)	28.4
Enstatite	19-768	(6 1 0)	31.1
Hexacelsian	26-0137	(1 0 1)	22.4
Celsian	38-1450	(2 2 0)	26.5
μ-Cordierite	14-249	(1 0 1)	25.8
Cristobalite	11-695	(1 0 1)	21.9

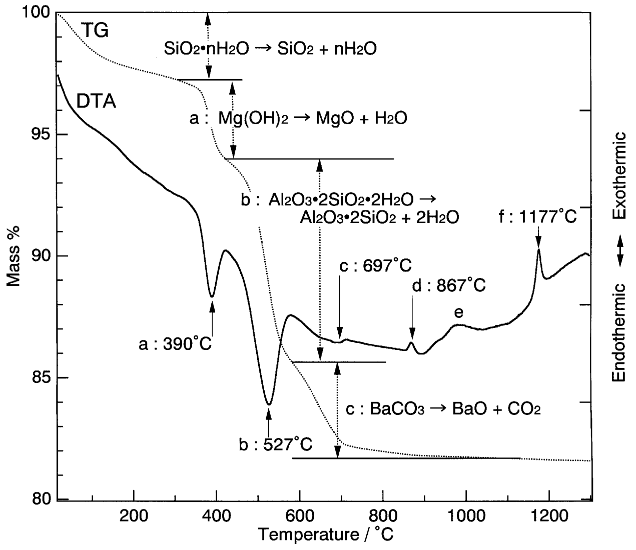

Fig. 3. DTA–TG curves of mixture $n = 0.333$, $m = 3$.

3. Results and discussions

3.1. Starting mixture with nominal composition of osumilite

3.1.1. Thermal analysis

Thermal analysis result of the nominal mixture ($n = 0.333$ and $m = 3$) is shown in Fig. 3. Four steps of weight loss are observed. The first weight loss below 300 °C relates to the dehydration of absorbed water by silica sol and kaolin. The second (300–400 °C) and the third (400–600 °C) mainly relate to the dehydration of $Mg(OH)_2$ and kaolin, respectively, and correspond to the endothermic peaks of DTA at 390 and 527 °C which agreed well with those reported in the previous paper [12]. The last weight loss between 600 and 800 °C relates to the decomposition of $BaCO_3$ and corresponds to the endothermic peak of DTA at 697 °C. Three exothermic peaks at 867, 1000, and 1177 °C will be discussed in the next section.

3.1.2. Sintering and crystallization characteristics

In Fig. 4(A), bulk density and apparent porosity of the sintered samples with the nominal composition of osumilite are plotted against heat treatment temperature. Changes in phase distribution with heat treatment temperature determined from X-ray diffraction on the same samples are also shown in Fig. 4(B) and (C). Sintering evaluated from bulk density and porosity proceeded broadly in following two stages, the first between 800 and 1000 °C and the second between 1100 and 1200 °C.

By comparing the results in Fig. 4, the following reaction processes could be assumed. MgO and BaO formed by the decomposition of raw materials $Mg(OH)_2$ and $BaCO_3$ at low temperature, reacted with dehydrated kaolin to form amorphous material below 800 °C, which promoted the densification by viscous flow below 1000 °C. From the X-ray diffraction patterns of specimens heat treated be-

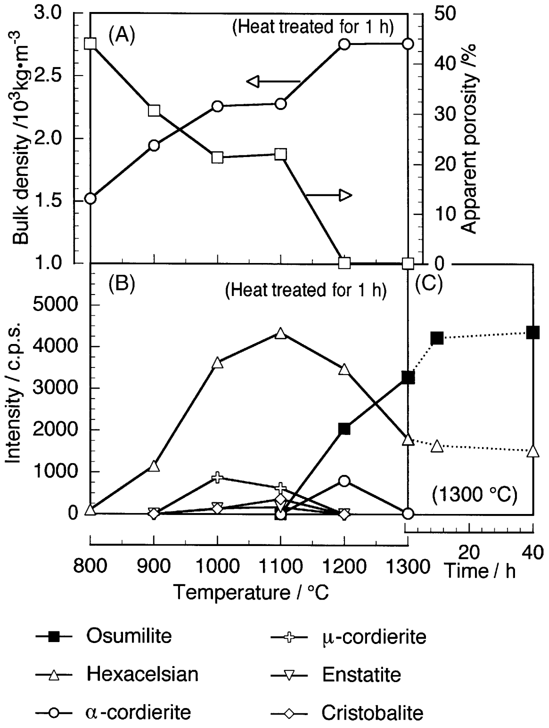

Fig. 4. Effect of heat treatment temperature on sintering and crystalline phases of specimen $n = 0.333$, $m = 3$.

low 1000 °C, in Fig. 5, the presence of the amorphous materials was clearly indicated by the broad peak around the diffraction angle of 20°–30°. The sinterability of the amorphous materials which were formed by the reaction of kaolin with alkaline-earth metal oxides, such as CaO, SrO, BaO, or MgO, have been already reported by authors [12–14]. Hexacelsian and μ-cordierite are thought to crystallize around the temperature which corresponded to the exothermic peak at 867 °C and the broad exothermic band around 1000 °C in the DTA curves of Fig. 3, respectively. Combined densification was suppressed by the development of a large amount of hexacelsian and μ-cordierite crystals at 1000 °C, which seemed to be caused by the disappearance of the amorphous-phase. At 1100 °C, Cristobalite was developed by crystallization of dehydrated silica, and enstatite was also developed by the reaction of silica with MgO.

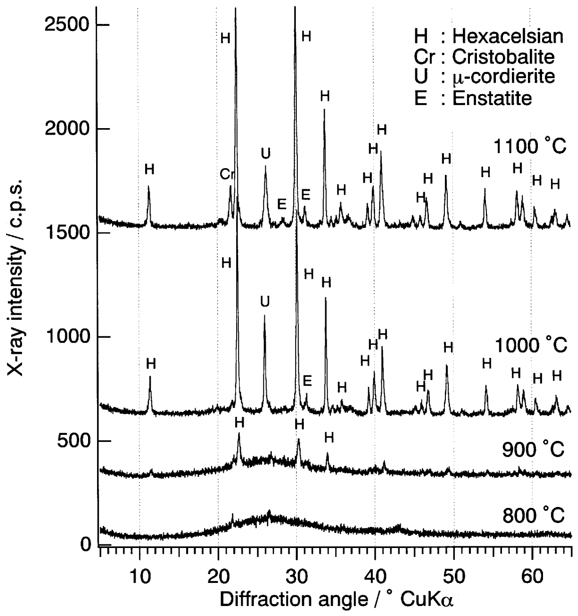

Fig. 5. X-ray diffraction patterns of specimens heat treated at respective temperatures.

Above 1100 °C, μ-cordierite, cristobalite and enstatite disappeared up to 1200 °C and hexacelsian gradually decreased, following the development of osumilite. Jais et al. [7] also reported that precursor phases, mullite, hexacelsian, or cordierite always started to crystallize at the initial stage, even though osumilite was the dominant-phase after 3 h at 1200 °C with other phases still present for the powders prepared by the sol–gel method. In addition, one of their sol–gel powders sintered in two stages just like the results in Fig. 4. The second densification was observed at a time from 1100 to 1200 °C. From the X-ray diffraction pattern of specimens heat treated at 1100 and 1200 °C, a broad peak around 20°–30°, which indicates the presence of amorphous materials, was not observed, so that the content of liquid-phase present at 1300 °C will be small. Although the detailed mechanisms are not clear, the driving force of the sintering is considered to be a materials transport accelerated by the phase change and a viscous flow of transiently formed small amount of liquid-phase.

Above 1200 °C, the formation of osumilite crystals increased with the decrease of hexacelsian and μ-cordierite. The transient α-cordierite-phase disappeared by 1300 °C. In this experiment, specimens were heat treated for just 1 h, so that the equilibrium state could not be exactly attained by the heat treatment even at 1300 °C. In order to further the crystallization reaction, heat treatments for long periods of time were performed at 1300 °C (Fig. 4(C)). Peak heights of osumilite and hexacelsian reached to constant values at more than 10 h of heat treatment.

Even for the mixture of nominal composition $2MgO\cdot BaO\cdot 3Al_2O_3\cdot 9SiO_2$, hexacelsian always coexisted with osumilite despite the prolonged heat treatment at high temperature. Lambrinou et al. [8] reported that the precursor crystals, cordierite and hexacelsian, formed prior to the crystallization of osumilite, still existed after heat treatment at high temperature. Winter et al. [15] also reported that single-phase osumilite ceramics was difficult to prepare because cordierite of varying Mg, Al, and Si ratios forms the remaining secondary phases. In order to estimate the availability of osumilite for thermal-shock resistant materials or electric insulating materials, it is necessary to prepare dense osumilite ceramics of single-crystalline-phase.

3.2. Starting mixture giving single-crystalline-phase of osumilite

3.2.1. Chemical composition for single-crystalline-phase osumilite

In order to prepare single-phase osumilite ceramics, effect of chemical composition ratio $n = \mathrm{MgO}/(\mathrm{MgO}+\mathrm{BaO})$ and $m = \mathrm{SiO_2}/\mathrm{Al_2O_3}$ on the phase assemblage was studied. The results are shown in Fig. 6. The experimental compositions in Fig. 6 correspond to the region of quadrilateral ABCD in Fig. 2, where three compounds, osumilite, cordierite, and celsian lie.

Osumilite crystals are observed in a wide compositional area of $0.2 < n < 0.8$ and $2.25 < m < 3.0$. On a left end line ($n = 0$) in Fig. 6, α-cordierite is always observed with spinel or cristobalite. On a right end line ($n = 1.0$), only hexacelsian is observed. Secondary phases always coexisted for all experimental compositions despite the prolonged heat treatments.

A detailed effect of molar ratio n on the X-ray peak intensity is shown in Fig. 7. All the specimens were heat treated at 1300 °C for 10 h. In a compositional area $n < 0.28$, α-cordierite is always formed though osumilite is predominant, and in a compositional area $n > 0.30$, hexacelsian and/or celsian crystals coexisted with predominant osumilite. Single-phase osumilite is obtained in a narrow compositional area $0.28 < n < 0.30$. Fig. 8 shows X-ray diffraction pattern of the specimen with $n = 0.29$, heat treated at 1300 °C. One was quickly taken out from the furnace kept at 1300 °C for 1 h, and another was allowed to cool down in the furnace after keeping for 40 h. Since the reaction of the former is insufficient, small diffraction peaks of hexacelsian and celsian was observed. When the peak heights of former were compared with those of latter, a small amount of glass-phase is thought to be remaining in a former specimen. Almost all the diffraction peaks of the latter were indexed as a hexagonal crystal structure of osumilite [3,14]. Although the presence of a small amount of liquid-phase at 1300 °C cannot be denied absolutely,

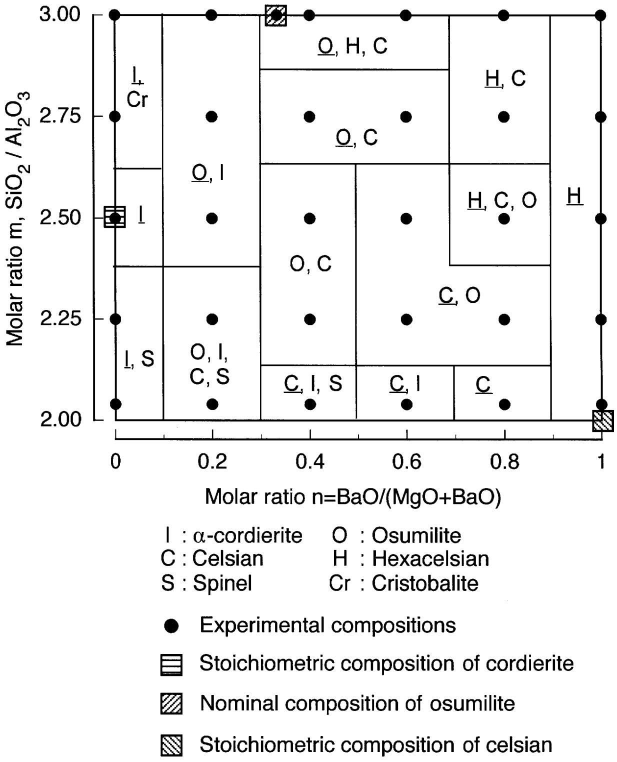

Fig. 6. Crystalline phases for specimens fired at 1300 °C for 10 h. Underline denotes predominant phases.

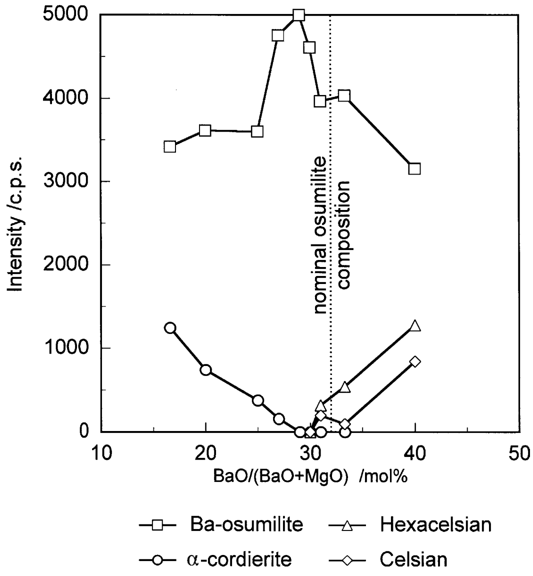

Fig. 7. Effect of molar ratio of MgO and BaO on the diffraction peak height for specimens heat treated at 1300 °C for 10 h.

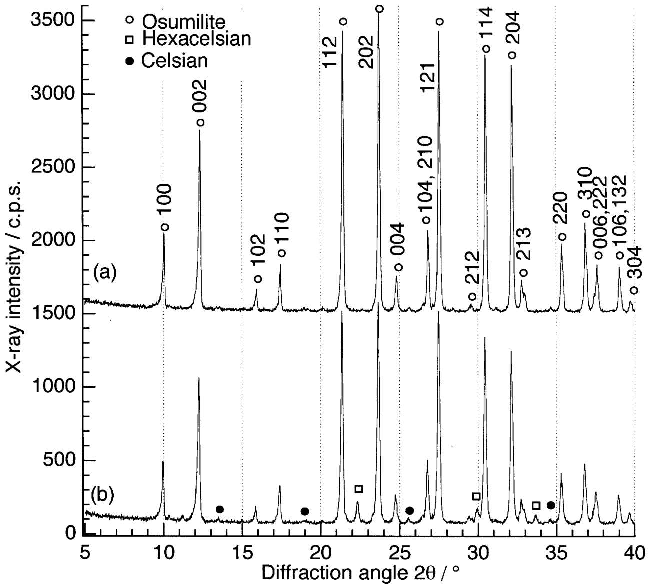

Fig. 8. X-ray diffraction pattern of specimen $n = 0.29$, $m = 3.0$. (a) Heat treated at 1300 °C for 40 h and then allowed to cool down. (b) Heat treated at 1300 °C for 1 h and then quenched.

Table 2
Chemical analysis of single-phase osumilite ceramics in Fig. 7

Component	Analysis		Nominal stoichiometric composition[b]	
	(mass%)	(mol)	(mass%)	(mol)
MgO	9.1	2.14	7.46	2.0
BaO	13.8	0.85	14.19	1.0
Al_2O_3	–	–	28.31	3.0
SiO_2	–	–	50.05	9.0
n[a]	–	0.283	–	0.333

[a] n equals to BaO/(MgO + BaO) in molar ratio.
[b] $2MgO \cdot BaO \cdot 3Al_2O_3 \cdot 9SiO_2$.

single-crystalline-phase of osumilite ceramics can be obtained in a very narrow compositional area.

In order to confirm the chemical composition giving single-crystalline-phase of osumilite, a chemical analysis of the single-phase specimen from the composition with $n = 0.29$ and reacted at 1300 °C for 40 h was performed by ICP spectrometry. The result shown in Table 2 reveals that the chemical composition giving single-crystalline-phase of osumilite is expressed as $2.14MgO \cdot 0.85BaO \cdot 3Al_2O_3 \cdot 9SiO_2$ in this work. Supplementary research concerning about a remaining glassy phase, which brings about compositional error, will be required using analytical microscopy to determine the deviation from the nominal composition of osumilite.

3.2.2. *Properties of single-crystalline-phase of osumilite ceramics*

Physical and electric properties of single-phase osumilite ceramics are summarized in Table 3. The bulk density of the single-crystalline-phase of osumilite ceramics, which were prepared at 1300 °C for 10 h, was 2.69×10^3 kg/m^3, and so the relative density to the ideal density reported, 2.805×10^3 kg/m^3 (JCPDS Card 16-402), was calculated to be 95.9%. The bulk density was higher than that obtained by sol–gel method [7]. In Fig. 9, SEM photograph of the above specimen shows that a small amount of tiny pores were observed on a polished section of dense osumilite ceramics obtained by a solid-state reaction of kaolin with synthesized ultrafine barium carbonate and magnesium hydroxide.

Table 3
Physical and dielectric properties of osumilite ceramics

Properties	
Bulk density ($\times 10^3$ kg/m^3)	2.69
Apparent porosity (%)	0.27
Relative density (%)	95.9
Thermal expansion coefficient ($\times 10^{-6}$/°C, RT–900 °C)	2.7
Dielectric constant	5.6 (at 1 MHz) 7.3 (at 9 GHz)
Dielectric loss (10^{-4})	0.5 (at 1 MHz) 2.2 (at 9 GHz)

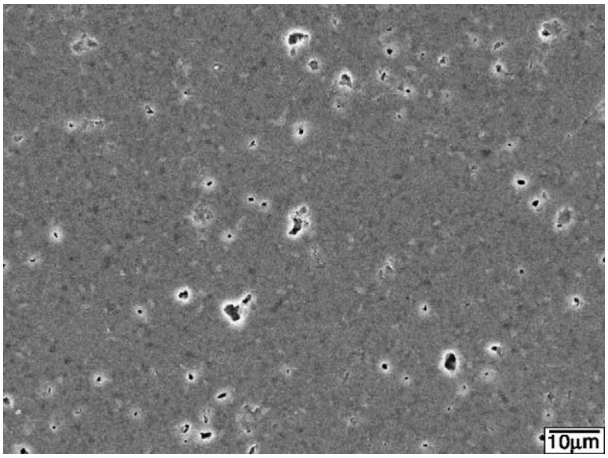

Fig. 9. SEM photograph of the polished section of a specimen $n = 0.29$, $m = 3.0$, heat treated at 1300 °C for 10 h.

As shown in Fig. 10, thermal expansion coefficient of single-crystalline-phase of osumilite ceramics was 2.7×10^{-6} K^{-1} from room temperature to 900 °C, which almost coincides with the value of Ba-celsian. Within this temperature range, osumilite expands twice as much as cordierite, but it is still low enough to give good thermal-shock resistance. Since the thermal expansion coefficient of osumilite is close to that of Si, dense osumilite ceramics is a candidate material for the application as the substrate of polycrystalline silicon solar cell.

As shown in Table 3, dielectric constant and dielectric loss of the single-phase osumilite ceramics are 5.6 and 5.0×10^{-5} at 1 MHz, respectively, which are half of that of alumina, so the osumilite ceramics can also be expected to exhibit high performances as a substrate material for high frequency integrated circuit. These dielectric properties are better than those of cordierite, and the thermal expansion coefficient of osumilite fits better for substrate materials good to high frequency electronic circuit or for fiber-reinforced ceramics matrix materials.

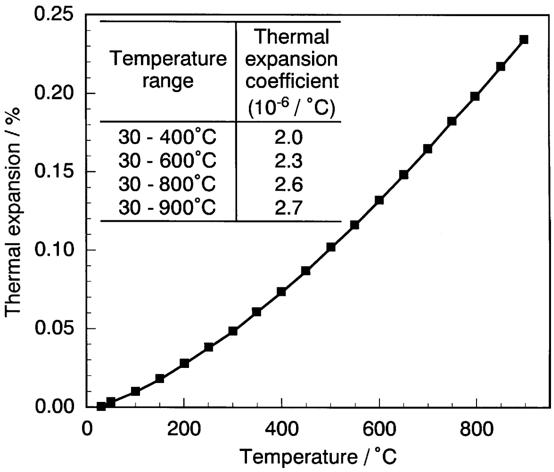

Fig. 10. Thermal expansion curve of single-phase osumilite.

4. Summary

In this study, dense ceramics of single-phase osumilite were obtained from the mixtures of synthesized ultrafine barium carbonate, magnesium hydroxide and submicron particles of kaolin by heat treatment at 1300 °C. Hexacelsian and cordierite crystallized first and then reacted with each other to form osumilite at prolonged heat treatment above 1200 °C. Single-phase osumilite ceramics is obtained at a molar ratio of 0.71/0.29 in MgO/BaO, near the nominal formula of osumilite $2MgO{\cdot}BaO{\cdot}3Al_2O_3{\cdot}9SiO_2$. Osumilite together with other silicates having low thermal expansion coefficients, such as cordierite and Ba-celsian exhibit excellent electric and thermal properties, so that the dense ceramics of single-phase osumilite are useful for the application as substrate materials for polycrystalline silicon solar cell or high frequency integrated circuit.

References

[1] R.S. Lamar, M.F. Warner, Reaction and fired-property studies of cordierite compositions, J. Am. Ceram. Soc. 37 (12) (1954) 602–610.

[2] A. Miyashiro, Osumilite, a new silicate mineral, and its crystal structure, Am. Miner. 41 (1956) 104–116.

[3] E. Gugel, H. Vogel, O. Osterried, Untersuchungen zur Verwendung von Bariumoxid enthaltenden Keramischen Massen als Steinzeug fur chemisch-technische Zwecke, Ber. Dtsch. Keram. Ges. 41 (9) (1964) 520–526.

[4] K.P. Gadkaree, K. Chyung, Silicon-carbide-whisker-reinforced glass and glass-ceramic composites, Am. Ceram. Soc. Bull. 65 (2) (1986) 370–376.

[5] S.M. Bleay, V.D. Scott, Effect of heat treatment in air on the structure and properties of barium osumilite reinforced with nicalon fibres, J. Mater. Sci. 27 (3) (1992) 825–838.

[6] C. Reich, R. Bruckner, Effect of preparation parameters on the properties of unidirectional SiC-fibre-reinforced MAS and BMAS glass-ceramics, Compos. Sci. Technol. 57 (1997) 533–541.

[7] U.S. Jais, W.E. Lee, P.F. James, Sol–gel preparation and crystallisation of barium osumilite glass, J. Non-Cryst. Solids 194 (1996) 213–224.

[8] K. Lambrinou, O. van der Biest, A.R. Boccaccini, D.M.R. Taplin, Densification and crystallisation behaviour of barium magnesium aluminosilicate glass powder compacts, J. Eur. Ceram. Soc. 16 (1996) 1237–1244.

[9] U.S. Jais, W.E. Lee, P.F. James, Crystallization of barium osumilite glass, J. Am. Ceram. Soc. 82 (11) (1999) 3200–3208.

[10] K. Sumi, Y. Kobayashi, E. Kato, Low-temperature fabrication of cordierite ceramics from kaolinite and magnesium hydroxide mixtures with boron oxide additives, J. Am. Ceram. Soc. 82 (4) (1999) 783–785.

[11] E.M. Levin, C.R. Robbins, H.F. McMurdie (Eds.), Phase Diagrams for Ceramists, The American Ceramic Society, 1964, p. 195, 246.

[12] K. Sumi, Y. Kobayashi, E. Kato, Synthesis and sintering of cordierite from ultrafine particles of magnesium hydroxide and kaolinite, J. Am. Ceram. Soc. 81 (4) (1998) 1029–1032.

[13] Y. Kobayashi, E. Kato, Low-temperature fabrication of anorthite ceramics, J. Am. Ceram. Soc. 76 (3) (1994) 833–834.

[14] Y. Kobayashi, K. Sumi, T. Asai, E. Kato, Fabrication of dense celsian ceramics by reaction of kaolin with $SrCO_3$ and $BaCO_3$, J. Ceram. Soc. Jpn. 107 (7) (1999) 657–661.

[15] W. Winter, C. Bogddanow, G. Muller, W. Pannhorst, Crystallization sequence of barium osumilite and MAS osumilite glass-ceramics with low thermal expansion, Glastech. Ber. 66 (5) (1993) 109–117.